J Math Chem (2015) 53:1207–1219
DOI 10.1007/s10910-015-0481-y

ORIGINAL PAPER

Probabilistic view of the luminescence phasor plot and description of the universal semicircle as the sum of two spiraling curves

Mário N. Berberan-Santos

Received: 6 December 2014 / Accepted: 9 February 2015 / Published online: 4 March 2015

Abstract Luminescence decay functions describe the time dependence of the intensity of radiation emitted by electronically excited species. Decay phasor plots (plots of the Fourier sine transform vs. the Fourier cosine transform, for one or several angular frequencies) are being increasingly used in fluorescence, namely in lifetime imaging microscopy. In this work it is shown that the universal semicircle, locus of all exponential decay functions, can be viewed as the weighted sum of two spiraling phasors, one corresponding to a truncated exponential and the other to a shifted exponential. The geometric details of this recomposition are discussed. With area normalization, the decay functions form a subset in the universe of one-sided probability density functions, the same being valid for the phasor plots, which are parametric plots of the respective characteristic functions.

Keywords Luminescence decay · Relaxation function · Characteristic function · Fourier transform · Spiral

Mathematics Subject Classification 42A38 · 14H81 · 60E10 · 78A10

1 Introduction

A *luminescence decay function*, $I(t)$, is the function describing the time dependence of the intensity of radiation spontaneously emitted at a given wavelength, by a previously excited sample. Only nonnegative times are considered ($t \geq 0$). For convenience, and without loss of generality, the decay function is usually normalized at $t = 0$, $I(0) = 1$

M. N. Berberan-Santos (✉)
CQFM - Centro de Química-Física Molecular and IN - Institute of Nanoscience and Nanotechnology, Instituto Superior Técnico, Universidade de Lisboa, 1049-001 Lisbon, Portugal
e-mail: berberan@tecnico.ulisboa.pt

(initial value normalization) [1,2]. A second normalization procedure (area normalization) is to consider instead the function

$$E(t) = \frac{I(t)}{\int_0^\infty I(t)\,dt}. \tag{1}$$

In this case, $E(t)$ can be called a *density* [3], as it has the properties of a probability density function (pdf). This definition has the advantage of including "decay" functions that start from zero, as occurs with the emission of intermediates and products of photochemical processes. The function $E(t)$ also has the meaning of the emission probability of a photon between t and $t + dt$, given that the photon was emitted.

The cosine and sine Fourier transforms of $E(t)$, $G(\omega)$ and $S(\omega)$, respectively, are defined by [1,4]

$$G(\omega) = \int_0^\infty \cos(\omega u) E(u)\,\mathrm{d}u, \tag{2}$$

$$S(\omega) = \int_0^\infty \sin(\omega u) E(u)\,\mathrm{d}u, \tag{3}$$

where ω is the angular frequency. Following Weber [5], the letter G is used instead of C (G is a convenient choice, as it avoids the concentration symbol while retaining graphic similarity with C).

Each decay function, for a given frequency, is mapped onto a point inside the unit circle defined by $G^2 + S^2 = 1$ [3,6], which may be said to be the *phasor space*, see Fig. 1. Indeed, Eqs. (2) and (3) immediately imply that both $|G|$ and $|S|$ cannot exceed 1. It also follows from these equations that $G(0) = 1$ and $S(0) = 0$, while $S(\infty) = G(\infty) = 0$, see Fig. 1.

For a given frequency, the (G, S) pair defines a point or, equivalently, a vector $\mathbf{P} = G\mathbf{e}_1 + S\mathbf{e}_2$, called the phase vector or *phasor*. This vector is the basis of the *phasor approach* to time-resolved luminescence (mainly fluorescence) [1,4,7–26], which provides a simple graphical and model-independent portrait of a system. Besides luminophore identification ("fingerprinting") in complex systems, processes such as quenching, solvent relaxation and energy transfer are defined by characteristic trajectories in the plane (at a fixed frequency or using several frequencies). Owing to the limited computational requirements, linearity and robustness, the phasor approach is especially useful in fluorescence lifetime imaging microscopy (FLIM) [11–14,18,21,22,25]. Application to measurements in solution ("single pixel data") is nevertheless also of interest [9,10,19,20,23].

The precise location of the decay in the plane, defined by its phasor, is a function of frequency and decay characteristics. Single exponential decays lie on a so-called *universal circle* (in fact a semicircle, for nonnegative frequencies), defined by $S = \sqrt{G(1-G)}$, with $1 \geq G \geq 0$ [1,4,7,12–14,19], see Fig. 1. Indeed, if

$$E(t) = \frac{1}{\tau}\exp\left(-\frac{t}{\tau}\right), \tag{4}$$

then Eqs. (2) and (3) give, as is well-known,

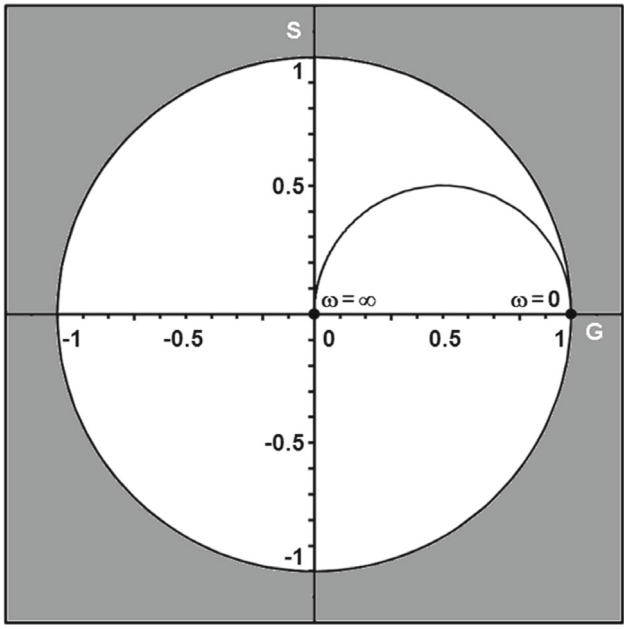

Fig. 1 The phasor space (*white area*) and the universal semicircle. Also shown are the (truly) universal points corresponding to all decay functions for zero and infinite frequencies. The universal semicircle, located in the first quadrant, defines the loci of all exponential decays. Other decay functions follow different paths between the two extreme points ($\omega = 0$ and $\omega = \infty$), when going from zero to infinite frequency

$$G(\omega) = \frac{1}{1 + (\omega\tau)^2}, \tag{5}$$

$$S(\omega) = \frac{\omega\tau}{1 + (\omega\tau)^2}. \tag{6}$$

Complex decays usually, but not always, fall inside the universal circle. The point corresponding to a multiexponential decay is located at an average distance from those of the components. In the case of a two-exponential decay with positive amplitudes, for instance, the corresponding point falls on a straight line connecting the phasors of the two components ("tie line") [1,4,7,19]. Analogously to the lever rule of thermodynamic phase diagrams, the fractional contribution of each of the two components to the total intensity is given by the length of the segment connecting the decay point ("average lifetime") to the opposite component, divided by the length of the full segment uniting the two extreme points (components) [1,4,12–14,18]. The lever rule was recently generalized to include cases where one of the amplitudes is negative [26]. When there are three or more components, again with positive amplitudes, the corresponding points define a polygon, with vertices located at or inside the circle, with the decay point lying in turn inside the polygon [1,4,11–13,18]. If some amplitudes are negative, the situation is different [26].

When the measurement technique used is frequency domain fluorimetry, based on sinusoidally modulated excitation, G and S are directly related to the two parameters obtained for each frequency, which are the modulation ratio, M, and the phase shift,

Φ, by $G = M\cos\Phi$ and by $S = M\sin\Phi$, hence $\tan\Phi = S/G$ and $M = |\mathbf{P}| = \sqrt{G^2 + S^2}$ [5]. When the measurement technique used is time domain fluorimetry, the phasor must be computed (numerically or analytically) from the measured decay according to Eqs. (2) and (3), at a conveniently chosen frequency (or set of frequencies). The decay is usually previously fitted with an empirical decay law, e.g. a sum of exponentials. An alternative procedure is discussed in Sect. 2.1.

As follows from Eqs. (2) and (3), $G(\omega)$ and $S(\omega)$ are not independent. They are explicitly related by Hilbert transforms [3],

$$G(\omega) = -\frac{2}{\pi}\int_0^\infty \frac{uS(u)}{\omega^2 - u^2}du, \tag{7}$$

$$S(\omega) = \frac{2\omega}{\pi}\int_0^\infty \frac{G(u)}{\omega^2 - u^2}du. \tag{8}$$

It might thus seem that a 2D plot would be redundant, as all information is already contained in $G(\omega)$. This nevertheless ignores the fact that a graphical representation that allows distinguishing between different decay types at a glance has intrinsic value, and also that in many cases experimental data is restricted to a few frequencies.

The purpose of the present work is to present a probabilistic view of the luminescence phasor approach and also to discuss the characteristic curve of the exponential luminescence decay function, the so-called universal circle, in terms of two components, which have more complex phasor plots.

2 Results and discussion

2.1 Probabilistic aspects

The functions $G(\omega)$ and $S(\omega)$ are the real and imaginary parts of the conjugate Fourier transform $F^*(\omega)$ of the decay function $E(t)$,

$$F^*(\omega) = \int_0^\infty E(t)e^{i\omega t}dt = G(\omega) + iS(\omega), \tag{9}$$

which is known in probability theory as the characteristic function (cf) of a given distribution, $\varphi(\omega)$ [6,27]. The phasor plot corresponding to the decay function $E(t)$, which is a pdf, can thus be viewed as a parametric plot of the respective characteristic function. When the pdf is symmetric, $S(\omega) = 0$ and the characteristic function is real [6]. A few complex characteristic functions of asymmetric distributions are given in [6] and in [27]. In the luminescence phasor context all pdfs are one-sided, hence the cf is generally complex. In the exponential case,

$$\varphi(\omega) = \frac{1}{1 - i\omega\tau}. \tag{10}$$

A further probabilistic aspect of the phasor plot approach exists in the case of luminescence data obtained by the single photon timing method [1]. In this case the luminescence decay is acquired as a histogram of photon counts, distributed by several narrow time intervals (channels). Neglecting for the sake of simplicity the convolution of the intrinsic decay with the instrument response function [1], assumed to be very short when compared to the characteristic decay times, the decay function is approximated by

$$E(t) = \sum_n f_n \delta(t - t_n), \tag{11}$$

where

$$f_n = \frac{N_n}{\sum_n N_n}, \tag{12}$$

N_n being the number of counts in the nth channel, corresponding to time t_n. The phasor plot can be obtained directly from the histogram. As the cf of $\delta(t - t_n)$ is $\exp(i\omega t_n)$, one has the approximate relations (which are but discrete Fourier transforms):

$$G(\omega) = \sum_n f_n \cos(\omega t_n), \tag{13}$$

$$S(\omega) = \sum_n f_n \sin(\omega t_n). \tag{14}$$

During the histogram acquisition period, the phasor curve will also evolve stochastically, converging to the final, stable form that corresponds to a large number of counts.

2.2 Universal semicircle as the sum of two spiraling curves

The simple phasor plot of exponential decays (universal circle, Fig. 1) can be expressed in terms of two other phasor curves, far more complex geometrically and bearing some similarities with previously discussed curves [26]. Indeed, the exponential can be broken into two parts, by splitting it at $\theta = \theta_0$ into the functions

$$I_L(\theta) = [1 - H(\theta - \theta_0)]\, e^{-\theta}, \tag{15}$$

$$I_R(\theta) = H(\theta - \theta_0) e^{-\theta}, \tag{16}$$

where $H(\theta)$ is the Heaviside step function. The decay function $I_L(\theta)$ is nonzero only to the left of θ_0, whereas the decay function $I_R(\theta)$ is nonzero only to the right of θ_0. After area normalization, yielding $E_R(\theta)$ and $E_L(\theta)$, they can be viewed as a "truncated exponential" and as a "shifted exponential", respectively. In this way,

$$G(u) = f_L G_L(u) + f_R G_R(u), \tag{17}$$

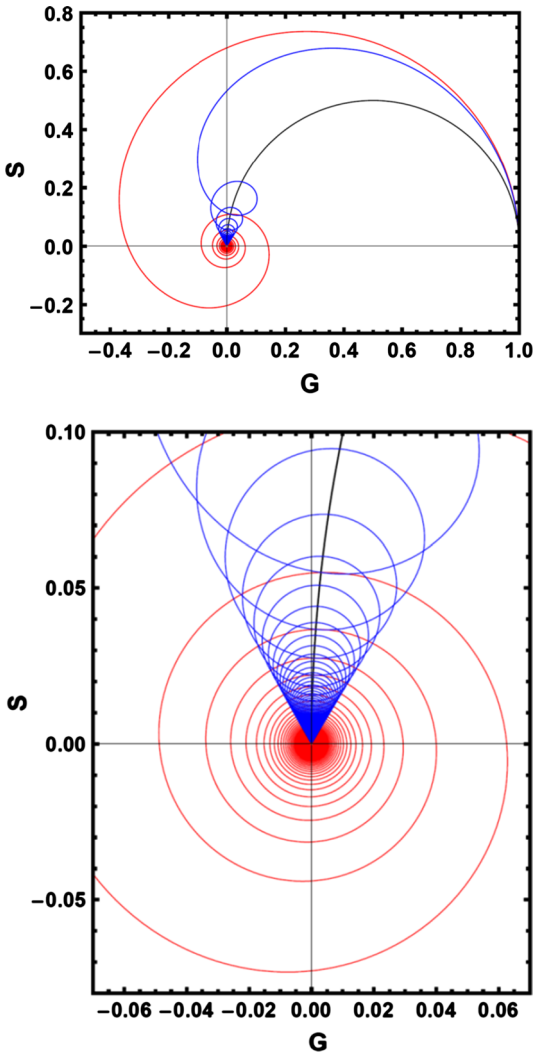

Fig. 2 Phasor plot for the exponential function ("universal semicircle"), including a zoom of the high frequency part, viewed as the sum of the phasors of Eqs. (15) and (16), in this example with $\theta_0 = \ln 2$. The phasor plot of the truncated exponential decay function, $E_L(\theta)$, is the *blue curve*, and the phasor plot of the shifted exponential decay function, $E_R(\theta)$, is the *red curve* (Color figure online)

$$S(u) = f_L S_L(u) + f_R S_R(u), \tag{18}$$

where f_L and $f_R = 1 - f_L$ are the relative contributions, with

$$f_L = \int_0^{\theta_0} e^{-\theta} d\theta = 1 - e^{-\theta_0}. \tag{19}$$

The cosine and sine transforms of the *truncated exponential* are:

$$G_L(u) = \frac{e^{\theta_0} + u \sin(\theta_0 u) - \cos(\theta_0 u)}{\left(e^{\theta_0} - 1\right)\left(1 + u^2\right)}, \tag{20}$$

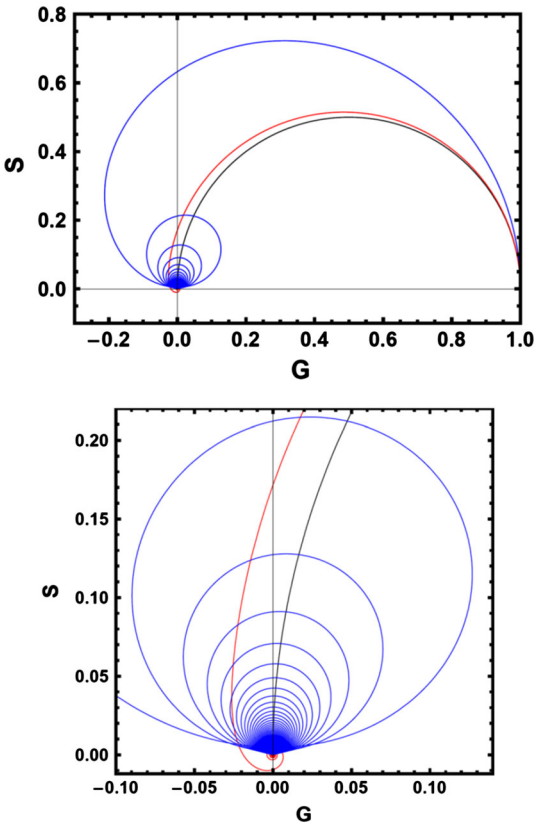

Fig. 3 Phasor plot for the exponential function ("universal semicircle"), including a zoom of the high frequency part, viewed as the sum of the phasors of Eqs. (15) and (16), in this example with $\theta_0 = 0.03$ ($f_L = 0.030$). The phasor plot of the truncated exponential decay function, $E_L(\theta)$, is the *blue curve*, and the phasor plot of the shifted exponential decay function, $E_R(\theta)$, is the *red curve* (Color figure online)

$$S_L(u) = \frac{e^{\theta_0} u - \sin(\theta_0 u) - u\cos(\theta_0 u)}{\left(e^{\theta_0} - 1\right)\left(1 + u^2\right)}, \tag{21}$$

while those of the *shifted exponential* are:

$$G_R(u) = \frac{\cos(\theta_0 u) - u\sin(\theta_0 u)}{1 + u^2}, \tag{22}$$

$$S_R(u) = \frac{u\cos(\theta_0 u) + \sin(\theta_0 u)}{1 + u^2}. \tag{23}$$

It follows from Eqs. (22) and (23) that for large u the phasor plot of the shifted exponential $E_R(\theta)$ becomes a hyperbolic spiral [28,29], with radius $1/u$ and polar angle (phase) $\theta_0 u$, see Fig. 2. This is similar to what was observed for the exponential of exponential decay function when unimodal [26]. On the other hand, the phasor path for the truncated exponential, $E_L(\theta)$, which has a singularity in the derivative at θ_0, is also an inward spiral, albeit distorted, reminiscent of the curves observed for some super-exponential decays [26]. For small θ_0 (Fig. 3) it is similar to the curve corresponding to a rectangular "decay"/pdf, which is of the cochleoid type [28,29]. As expected, for small θ_0 the cf *of* $E_L(\theta)$ becomes similar to the universal semicircle,

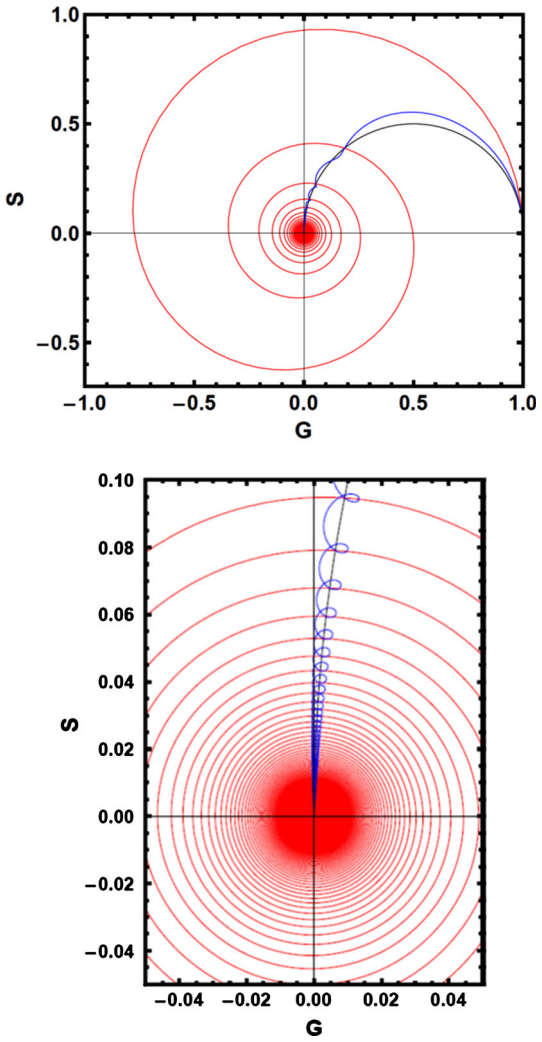

Fig. 4 Phasor plot for the exponential function ("universal semicircle"), including a zoom of the high frequency part, viewed as the sum of the phasors of Eqs. (15) and (16), in this example with $\theta_0 = 3$ ($f_L = 0.95$). The phasor plot of the truncated exponential decay function, $E_L(\theta)$, is the *blue curve*, and the phasor plot of the shifted exponential decay function, $E_R(\theta)$, is the *red curve* (Color figure online)

whereas for large θ_0 this happens to the cf of $E_R(\theta)$, which nearly loses the convoluted character, see Figs. 3 and 4, respectively.

It also follows from Eqs. (20)–(23) that the R and L phasors coincide exactly for $u = 2n\pi/\theta_0$ ($n = 1, 2, \ldots$), see e.g. Figs. 6, 8 and 10.

The full circle can be obtained in the same way, if negative frequencies are also used, Fig. 11.

The shifted exponential curve (red curve) is also directly related to the curve of the unshifted exponential (universal circle), as Eqs. (22) and (23) can be rewritten in the form

$$\begin{bmatrix} G_R(u) \\ S_R(u) \end{bmatrix} = \begin{bmatrix} \cos(\theta_0 u) & -\sin(\theta_0 u) \\ \sin(\theta_0 u) & \cos(\theta_0 u) \end{bmatrix} \begin{bmatrix} \frac{1}{1+u^2} \\ \frac{u}{1+u^2} \end{bmatrix}, \tag{24}$$

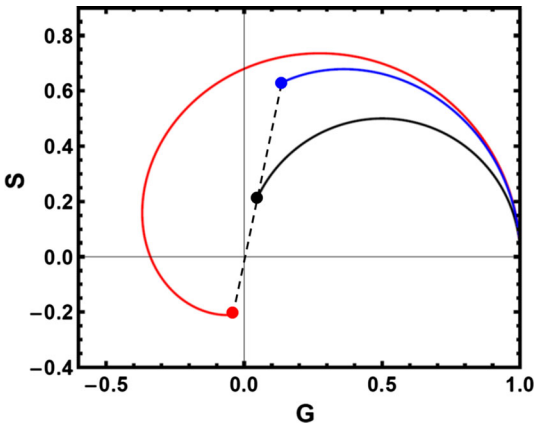

Fig. 5 Phasor plot for the exponential function ("universal semicircle"), viewed as the weighted sum of the phasors of Eqs. (15) and (16), with $\theta_0 = \ln 2$. The phasor plot of the truncated exponential decay function, $E_L(\theta)$, is the *blue curve*, and the phasor plot of the shifted exponential decay function, $E_R(\theta)$, is the *red curve*. The lever rule ($f_L = 1/2$) is shown for a reduced frequency $u = \pi / \ln 2$ (Color figure online)

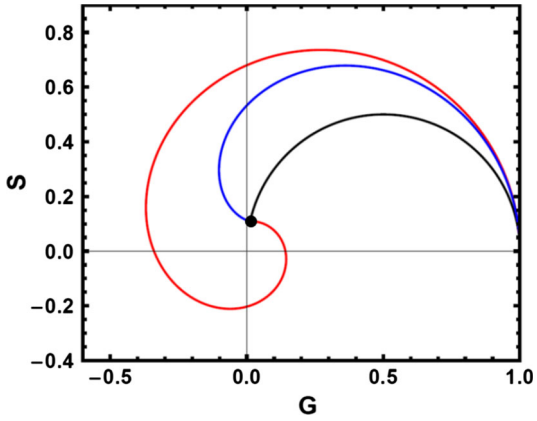

Fig. 6 Phasor plot for the exponential function ("universal semicircle"), viewed as the sum of the phasors of Eqs. (15) and (16), with $\theta_0 = \ln 2$. The phasor plot of the truncated exponential decay function, $E_L(\theta)$, is the *blue curve*, and the phasor plot of the shifted exponential decay function, $E_R(\theta)$, is the *red curve*. For the depicted reduced frequency, $u = 2\pi / \ln 2$, the *two curves* meet at the same point (Color figure online)

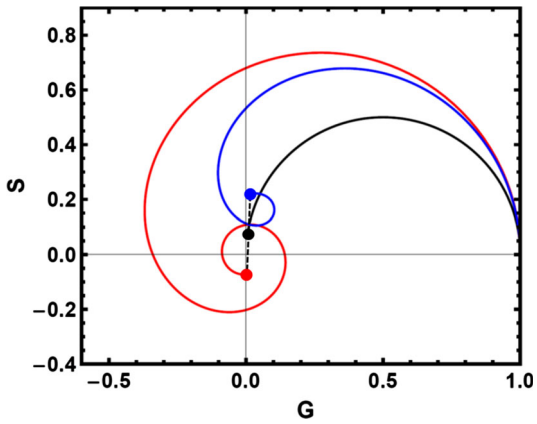

Fig. 7 Phasor plot the exponential function ("universal semicircle"), viewed as the sum of the phasors of Eqs. (15) and (16), with $\theta_0 = \ln 2$. The phasor plot of the truncated exponential decay function, $E_L(\theta)$, is the *blue curve*, and the phasor plot of the shifted exponential decay function, $E_R(\theta)$, is the *red curve*. The lever rule ($f_L = 1/2$) is shown for a reduced frequency $u = 3\pi / \ln 2$ (Color figure online)

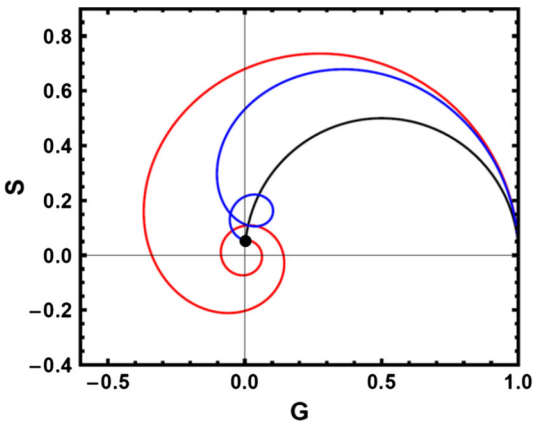

Fig. 8 Phasor plot the exponential function ("universal semicircle"), viewed as the sum of the phasors of Eqs. (15) and (16), with $\theta_0 = \ln 2$. The phasor plot of the truncated exponential decay function, $E_L(\theta)$, is the *blue curve*, and the phasor plot of the shifted exponential decay function, $E_R(\theta)$, is the *red curve*. For the depicted reduced frequency, $u = 4\,\pi\,/\ln 2$, the *two curves* meet at the same point (as in Fig. 5) (Color figure online)

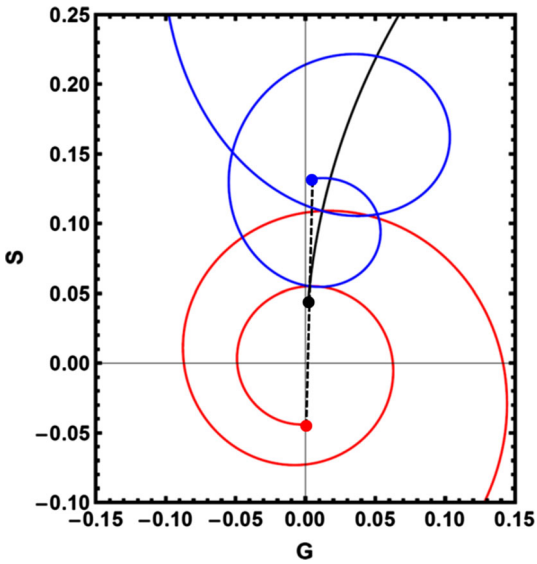

Fig. 9 Phasor plot the exponential function ("universal semicircle"), viewed as the sum of the phasors of Eqs. (15) and (16), with $\theta_0 = \ln 2$. The phasor plot of the truncated exponential decay function, $E_L(\theta)$, is the *blue curve*, and the phasor plot of the shifted exponential decay function, $E_R(\theta)$, is the *red curve*. The lever rule ($f_L = 1/2$) is shown for a reduced frequency $u = 5\,\pi\,/\ln 2$ (Color figure online)

which corresponds to a rotation of the original vector by an angle $\theta_0 u$, as can be seen in Figs. 5, 6, 7, 8, 9 and 10 (where the effective rotation is either π or 2π). This result is a special case of the shift property of causal functions (functions $f(t)$ such that $f(t) = 0$ if $t < 0$ [3]), which is demonstrated in the Appendix.

The decomposition of the exponential decay function can also be made with three or more functions, overlapping or not in time.

3 Conclusions

With the area normalization expressed by Eq. (1), the luminescence decay functions $E(t)$ form a subset in the universe of all one-sided probability density functions,

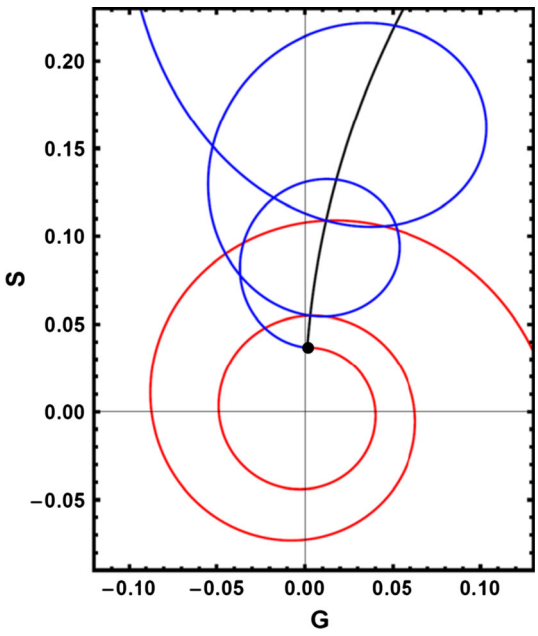

Fig. 10 Phasor plot the exponential function ("universal semicircle"), viewed as the sum of the phasors of Eqs. (15) and (16), with $\theta_0 = \ln 2$. The phasor plot of the truncated exponential decay function, $E_L(\theta)$, is the *blue curve*, and the phasor plot of the shifted exponential decay function, $E_R(\theta)$, is the *red curve*. For the depicted reduced frequency, $u = 6\,\pi\,/\ln 2$, the *two curves* meet at the same point (as in Figs. 5, 7) (Color figure online)

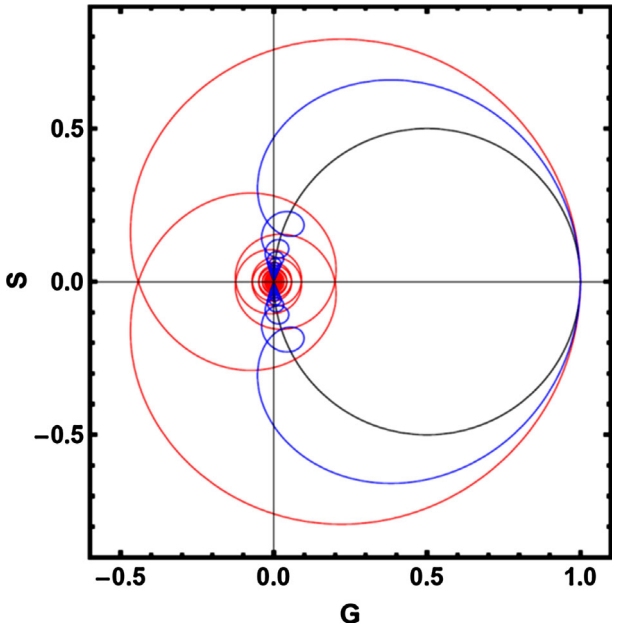

Fig. 11 Reconstruction of the *full circle*, viewed as the sum of the phasors of Eqs. (15) and (16), with $\theta_0 = \ln 2$. Both positive and negative frequencies are used. The phasor plot of the truncated exponential decay function, $E_L(\theta)$, is the *blue curve*, and the phasor plot of the shifted exponential decay function, $E_R(\theta)$, is the *red curve*. *Both curves* start ($u = -\infty$) and end ($u = +\infty$) at the origin, and evolve counterclockwise as the frequency increases (Color figure online)

the same being valid for the phasor plots, which are parametric plots of the respective characteristic functions. Decomposition of the exponential decay function in two non-overlapping functions (truncated exponential and shifted exponential) allowed retrieving phasor plots similar to those previously obtained for super-exponential and unimodal functions.

Acknowledgments This work was carried out within Projects PTDC/QUI-QUI/123162/2010 and RECI/CTM-POL/0342/2012 (FCT, Portugal).

Appendix: Shift property of causal functions

If a given causal function $f(t)$ is shifted to the right by Δt, it becomes another causal function $g(t) = f(t - \Delta\mathrm{t})$. The Fourier cosine transform of $g(t)$ is, successively,

$$G[g] = \int_0^\infty \cos(\omega t) g(t) dt = \int_0^\infty \cos(\omega t) f(t - \Delta t) dt = \int_0^\infty \cos(\omega t' + \omega \Delta t) f(t') dt', \tag{25}$$

hence

$$G[g] = \cos(\omega \Delta t) G[f] - \sin(\omega \Delta t) S[f]. \tag{26}$$

Similarly, it is obtained that

$$S[g] = \sin(\omega \Delta t) G[f] + \cos(\omega \Delta t) S[f], \tag{27}$$

and therefore

$$\begin{bmatrix} G[g] \\ S[g] \end{bmatrix} = \begin{bmatrix} \cos(\omega \Delta t) & -\sin(\omega \Delta t) \\ \sin(\omega \Delta t) & \cos(\omega \Delta t) \end{bmatrix} \begin{bmatrix} G[f] \\ S[f] \end{bmatrix} \tag{28}$$

A time shift Δt is tantamount to a counter-clockwise rotation by $\omega \Delta t$ in the phasor space.

References

1. B. Valeur, M.N. Berberan-Santos, *Molecular Fluorescence. Principles and Applications*, 2nd edn. (Wiley-VCH, Weinheim, 2012)
2. M.N. Berberan-Santos, B. Valeur, J. Lumin. **126**, 263 (2007)
3. A. Papoulis, *The Fourier Integral and Its Applications* (McGraw-Hill, New York, 1962)
4. D.M. Jameson, *Introduction to Fluorescence* (CRC Press, Boca Raton, 2014)
5. G. Weber, J. Phys. Chem. **85**, 949 (1981)
6. W. Feller, *An Introduction to Probability Theory and its Applications*, vol. II, 2nd edn. (Wiley, New York, 1971)
7. D.M. Jameson, E. Gratton, R.D. Hall, Appl. Spectrosc. Rev. **20**, 55 (1984)
8. M. Berberan-Santos, J. Lumin. **50**, 83 (1991)

9. M. Itagaki, K. Watanabe, Bunseki Kagaku **43**, 1143 (1994)
10. M. Itagaki, M. Hosono, K. Watanabe, Anal. Sci. **13**, 991 (1997)
11. P.J. Verveer, P.I.H. Bastiaens, J. Microsc. **209**, 1 (2003)
12. A.H.A. Clayton, Q.S. Hanley, P.J. Verveer, J. Microsc. **213**, 1 (2004)
13. G.I. Redford, R.M. Clegg, J. Fluoresc. **15**, 805 (2005)
14. M.A. Digman, V.R. Caiolfa, M. Zamai, E. Gratton, Biophys. J. **94**, L14 (2008)
15. A.H.A. Clayton, J. Microsc. **232**, 306 (2008)
16. Y.-C. Chen, R.M. Clegg, Photosynth. Res. **102**, 143 (2009)
17. Y.-C. Chen, B.Q. Spring, C. Buranachai, G. Malachowski, R.M. Clegg, Proc. SPIE **7183**, 718302 (2009)
18. C. Stringari, A. Cinquin, O. Cinquin, M.A. Digman, P.J. Donovan, E. Gratton, Proc. Natl. Acad. Sci. USA **108**, 13582 (2011)
19. M. Stefl, N.G. James, J.A. Ross, D.M. Jameson, Anal. Biochem. **410**, 62 (2011)
20. N.G. James, J.A. Ross, M. Stefl, D.M. Jameson, Anal. Biochem. **410**, 70 (2011)
21. E. Hinde, M.A. Digman, C. Welch, K.M. Hahn, E. Gratton, Microsc. Res. Tech. **75**, 271 (2012)
22. M.A. Digman, E. Gratton, in *Fluorescence Lifetime Spectroscopy and Imaging: Principles and Applications in Biomedical Diagnostics* (L. Marcu, P.M.W. French, and D.S. Elson eds., CRC Press, Boca Raton, 2012)
23. F. Menezes, A. Fedorov, C. Baleizao, B. Valeur, M.N. Berberan-Santos, Methods Appl. Fluoresc. **1**, 015002 (2013)
24. E. Hinde, M.A. Digman, K.M. Hahn, E. Gratton, Proc. Natl. Acad. Sci. USA **110**, 135 (2013)
25. Y. Engelborghs, A.J.W.G. Visser (eds.), *Fluorescence Spectroscopy and Microscopy* (Humana Press, New York, 2014)
26. M.N. Berberan-Santos, Chem. Phys. **449**, 23 (2015)
27. A. Stuart, K. Ord, *Kendall's Advanced Theory of Statistics*, vol. 1, 6th edn. (Hodder Arnold, London, 1994)
28. F.G. Teixeira, *Traité des Courbes Spéciales Remarquables Planes et Gauches, Tome II* (Coimbra University Press, Coimbra, 1908)
29. J.D. Lawrence, *A Catalogue of Special Plane Curves* (Dover, Mineola, 1972)